

Atomically-resolved imaging by frequency-modulation atomic force microscopy using a quartz length-extension resonator

Toshu An

The Institute for Solid State Physics, The University of Tokyo and PRESTO, Japan Science and Technology Agency, 5-1-5 Kashiwa-no-ha, Kashiwa 277-8581, Japan

Toyoaki Eguchi

The Institute for Solid State Physics, The University of Tokyo, 5-1-5 Kashiwa-no-ha, Kashiwa 277-8581, Japan

Kotone Akiyama and Yukio Hasegawa^{a)}

The Institute for Solid State Physics, The University of Tokyo, and PRESTO, Japan Science and Technology Agency, 5-1-5 Kashiwa-no-ha, Kashiwa 277-8581, Japan

(Received 13 May 2005; accepted 5 August 2005; published online 22 September 2005)

Using a 1 MHz length-extension type of quartz resonator as a force sensor for frequency-modulation atomic force microscopy (AFM), atomically resolved images of the Si(111)-(7×7) surface was obtained. Fabrications of a tip attached at the front end of the resonator by focused ion beam, and removal of the native oxide layer on the tip by in-situ field ion microscopy are found effective for achieving the highly-resolved AFM imaging. © 2005 American Institute of Physics. [DOI: 10.1063/1.2061850]

In atomic force microscopy (AFM), several kinds of sensors are used for detecting forces from the sample surface and making images of various properties in nanometer-scale spatial distributions. Among them a resonator made of quartz crystal has several unique advantages. A self-sensing capability due to a piezoelectric property of quartz eliminates the need of complicated optical alignments, which are required in the interferometric or optical lever methods using a conventional cantilever.¹ The simple configuration facilitates its applications, e.g., to experiments in low temperature.^{2,3} With its high quality factor (Q factor) regardless of the environment, it can be utilized not only in vacuum conditions but also in air and liquid,⁴ e.g., for biological applications.

In frequency modulation AFM (FM-AFM), where the force from the sample surface is detected as a shift of the resonance frequency of sensors, one can operate quartz resonators with a small oscillation amplitude because of its high stiffness without snapping a tip attached on the resonator into the sample ("jump to contact"). It has been known that in the FM-AFM the small oscillation effectively detects short-range forces, which contributes to atomic resolution in AFM imaging.^{5,6}

Making use of advantages of quartz, Giessibl demonstrated atomically resolved FM-AFM imaging on the Si(111)-(7×7) surface using a quartz tuning fork (qPlus sensor),⁷ whose resonance frequency is ≈ 30 kHz. Heike and Hashizume also reported the atomically resolved imaging using a quartz length-extension resonator (LER) in a phase-shift detection method,⁸ different from the FM method. In the phase method, a bandwidth of the force detection is limited by $Q/\pi f_0$ where f_0 is the resonant frequency while the FM method is not.⁹

In the present study, we carried out the FM-AFM experiment using an LER. It has rather high resonance frequency, 1 MHz, advantageous for obtaining additional properties us-

ing the modulation technique. A tungsten tip attached on LER was fabricated for an AFM probe with focused ion beam (FIB).¹⁰ Prior to the AFM observations, field ion microscopy (FIM) observation of the W tip was performed *in situ* to remove oxide layer covering the tip. Then using the probe highly-resolved topographic imaging of the Si(111)-(7×7) surface was achieved for the first time in the FM-mode of AFM.

A photograph of the LER used in this experiment is shown in Fig. 1(a). The LER, which was made by Micro Crystal, has a quartz rod with a dimension of 2.76 mm in length, 70 μm in width and 130 μm in thickness.^{8,11} The rod is supported with two arms at the center and the arms are connected to a base plate. Each side of the rod is coated with an Au electrode, as illustrated in Fig. 1(b). The base plate was glued on a sensor holder with insulating epoxy and each electrode on the rod was electrically connected to an electrode on the holder by conductive silver epoxy paste.

As shown in the scanning electron microscopy (SEM) image of Figs. 1(c) and 1(d), a W wire of 5 or 10 μm in diameter was glued with silver epoxy on the apex of the LER rod. The electrical contact was made between the W tip and the left-side electrode by the conductive epoxy. The wire was then sharpened by FIB. The method of the tip sharpening is basically same as reported in our previous paper.¹⁰ Figure 1(e) shows a zoomed SEM image of the sharpened W tip. The W tip can be repeatedly sharpened by FIB with a tip radius less than 10 nm.¹⁰

The resonance oscillation of the LER was stimulated in the two methods: one is applying a sinusoidal voltage on one of the two electrodes on the rods (electrical oscillation) and the other is applying the same voltage on a piezo actuator attached below the resonator (mechanical oscillation) [see Fig. 2(a)]. When the rod is extended or contracted, electronic charges due to the piezoelectric effect are induced on the surface of its side walls. The induced charges are detected as a current from an electrode on the rod and a voltage signal

^{a)} Author to whom correspondence should be addressed; electronic mail: hasegawa@issp.u-tokyo.ac.jp

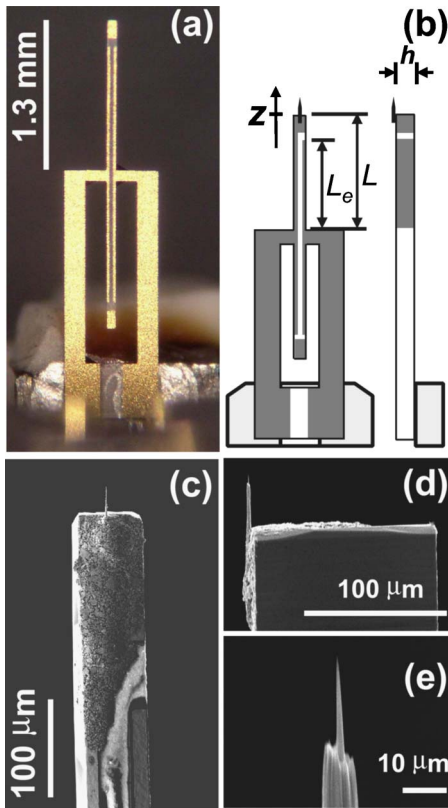


FIG. 1. (Color online) (a) A photograph of a force sensor used in this study (without tip): the base part of an LER is attached onto a sensor holder with separated electrical contacts, as shown in the schematic drawing of (b). The central rod oscillates in the z direction in a manner symmetric to the supporting points. (c) A SEM image of the rod apex with a W tip. (d) A side view of the rod apex. (e) A SEM image of the W tip fabricated by FIB.

converted by a preamplifier (OPA637AP with a $10\text{ M}\Omega$ feedback resistance) is fed into an automatic gain controller to stimulate the resonance and to keep the oscillation amplitude constant. The output of the preamplifier is also connected to an FM demodulator to obtain the amount of a shift of the

resonance frequency, which is a representative value of force acting on the tip from the sample surface.

In the experiments we used Omicron ultrahigh vacuum (UHV) STM/AFM system⁶ with a modification so that both electrodes of the resonator are electrically connected to the outside of the UHV chamber. One may notice in a schematic diagram of Fig. 2(a) that the frequency shift signal (Δf) is filtered with a low pass filter (LPF) of $\sim 300\text{ Hz}$, and is rectified with an absolute amplifier before fed into the AFM feedback circuit as a regulating signal of the tip-sample distance. The rectification of the Δf signal with the absolute amplifier prevents the tip from severe crash onto the sample when the attractive force diminishes. The tip position can be stabilized in a regime of repulsive force when the attractive force becomes smaller than the amount set by the AFM feedback controller.¹² The tunneling current can be measured using another preamplifier attached to the sample.

The amount of the current induced by the LER oscillations can be estimated as follows.⁷ When the resonator oscillates with its resonance frequency f_0 and oscillation amplitude A_0 , the displacement z of the rod apex is given by $z(t) = A_0 \sin(2\pi f_0 t)$. The strain ε in the rod at a position of l measured from the supporting point is given by

$$\varepsilon(t) = \frac{\pi A_0}{2L} \sin \frac{l\pi}{2L} \sin 2\pi f_0 t = \frac{\pi}{2L} z \sin \frac{l\pi}{2L},$$

where L is a length of the upper part of the rod [1.34 mm for the LER, see Fig. 1(b)]. This strain causes stress σ , which is given by $\sigma = \varepsilon E$, where E is Young's modulus ($7.8 \times 10^{10}\text{ N/m}^2$ for quartz in the direction of LER). Then the stress induces charge on the rod surface with an area density given by $\rho = \sigma d_{31}$, where d_{31} is the piezoelectric coupling constant ($2.31 \times 10^{-12}\text{ C/N}$ for quartz⁷). The induced charge on one side of the electrodes is calculated by integrating ρ over its area, which is given by

$$q(t) = 2h \int_0^{L_e} \rho = 2Ed_{31}h \left(1 - \cos \frac{L_e\pi}{2L}\right) z(t).$$

Here h is a thickness of the rod and L_e is a length of the upper electrode [1.10 mm for the LER, see Fig. 1(b)]. Sensitivity of the current to the displacement of the rod apex or the oscillation amplitude $S_{\text{cal}} = (dq/dt)/z$ is given by

$$S_{\text{cal}} = 4\pi f_0 Ed_{31}h \left(1 - \cos \frac{L_e\pi}{2L}\right).$$

With $f_0 = 997\,406\text{ Hz}$, we find $S_{\text{cal}} = 210\text{ nA/nm}$. The experimentally measured sensitivity was 125 nA/nm . The lower value of the sensitivity than the theoretical one is presumably due to non-ideal effect at the edges of the electrodes.⁷

The typical resonance curves obtained by the electrical and mechanical oscillation methods are shown in Figs. 2(b) and 2(c). Both curves, taken in UHV condition, exhibit a strong resonance peak. In addition, the electrical curve has a dip due to the anti-resonance at higher frequency. We noticed that Q factor of the mechanical one tend to be higher ($\sim 50\,000$) than that of the electrical one ($\sim 45\,000$). The Q factor measured in air is $\approx 20\,000$, still high compared with conventional silicon cantilevers.

The W tip, attached on the rod and sharpened by FIB, was then prepared and characterized *in situ* with FIM. The FIM is composed of a counter electrode with a tiny hole, the FIM is composed of a counter electrode with a tiny hole,

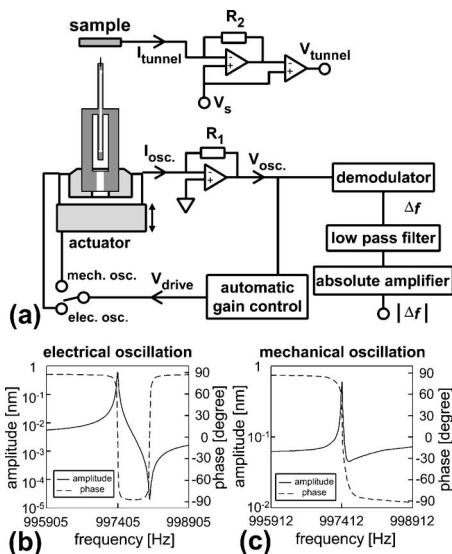


FIG. 2. (a) A schematic of the sensor part of AFM and the FM-AFM detection system. (b) and (c) The typical resonant curves of the LER by electrical (b) and mechanical (c) oscillation method. The measured resonance frequency f_0 and Q factor are $997\,403\text{ Hz}$ and $47\,172$ for the electrical oscillation, and $997\,412\text{ Hz}$ and $51\,479$ for the mechanical one, respectively.

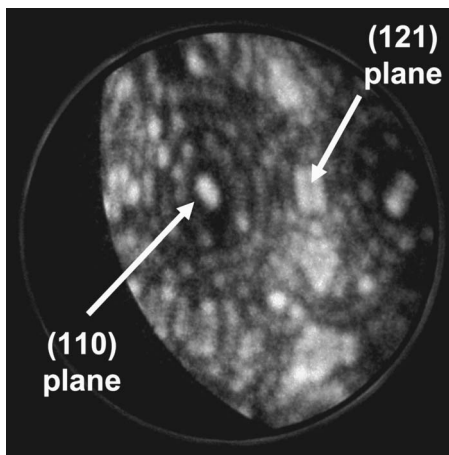


FIG. 3. A FIM image obtained with a W tip attached on the LER (imaging gas: He, applied voltage: ~ 4 kV). During the observation the tip was kept at room temperature.

microchannel plate and screen.¹³ For the imaging, we applied $+0.5 \sim 1$ kV on the tip and a negative voltage on the counter-electrode to make a strong electrical field on the tip apex. The FIM observation was performed until the native oxide layer on the tip is removed by field evaporation and a crystalline pattern of bare W tip appears. A typical FIM image of a W tip attached on the LER apex showing the (110)-oriented bcc-metal pattern is presented in Fig. 3. The tip radius of a W tip can be estimated from the FIM image by counting the number of atomic layers between two planes shown in the image.¹⁴ For instance, if n (110) layers are found between the (110) and (121) planes in a FIM image, the radius is given by $0.167n$ (nm). In the FIM image shown in Fig. 3, 5–6 layers are observed between the two planes, and thus the radius is 9 nm. The tip radius just after the removal of the oxide layer was measured 5–6 nm. We found that the FIM treatment is quite effective to obtain atomically resolved AFM images. So far, the preparation or characterization of the AFM tip *in situ* by FIM has been quite difficult because of the peculiar tip position on the conventional cantilevers. The straight alignment of the LER rod and tip, however, makes them possible. We believe that the capability of the *in situ* tip preparation and characterization by FIM is another great advantage of LER for a sensor of AFM.

Using the tip prepared with FIM, a force curve, i.e., a plot of Δf as a function of the tip-sample distance was measured on the Si(111)-(7 \times 7) surface, as is shown in Fig. 4(a). It was measured in a UHV condition with the oscillation amplitude of 0.75 nm. The oscillation amplitude is quite small compared with the cases of the Si cantilevers, which was 2–4 nm in our previous observations.^{6,15} The small amplitude was made possible by the high stiffness of the LER (540 000 N/m). The measured minimum normalized frequency shift is ca. -3 fN m^{1/2}, rather small compared with the previous results,^{6–8} indicating small van der Waals force acting on the tip. The small long-range force is due to the small oscillation amplitude and the sharpened tip by FIB. By reducing the long-range force and preferentially detecting the short-range chemical bonding force,⁶ the atomically resolved image of the surface was taken, as is shown in Fig. 4(b). The adatom structure on the surface and defects are clearly resolved in the FM-AFM image, demonstrating high performance of the LER.

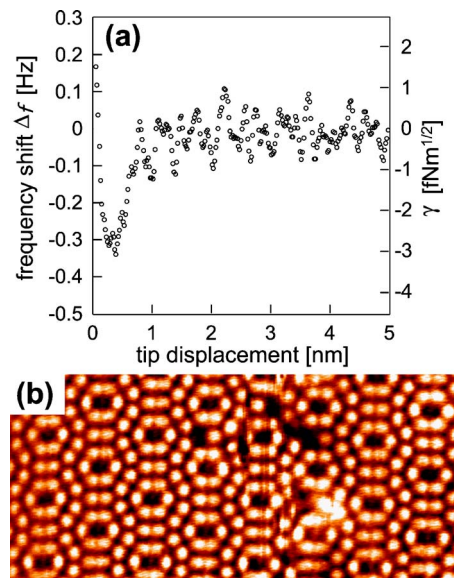


FIG. 4. (Color online) (a) A force curve taken with the LER on the Si(111)-(7 \times 7) surface (oscillation amplitude A_0 : 0.75 nm, resonance frequency f_0 : 997 406 Hz). γ , on the right vertical axis means normalized frequency shift, which is equal to $kA_0^{3/2}\Delta f/f_0$. k is a force constant of the LER, which is 540 000 N/m. (b) A FM-AFM image of the Si(111)-(7 \times 7) surface obtained by the electrical oscillation method. The observed area is 19 nm \times 9 nm. f_0 : 997 406 Hz, Δf : -0.37 Hz, A_0 : 0.75 nm, sample bias: $+0.5$ V, scan speed: 40 nm/s, LPF: fourth order with a cutoff frequency of 284 Hz.

In summary, a 1 MHz length-extension quartz resonator was used as a force sensor of AFM. By using FM detection method highly resolved Si image was successfully taken. The sharpening of the W tip with FIB and the removal of the oxide layer on the tip by *in situ* FIM are found effective for the stable operation in the AFM experiments.

The authors appreciate Tomihiro Hashizume, Seiji Heike, Bruno Studer, and Masami Kageshima for fruitful discussion and technical assistance.

¹W. Allers, A. Schwartz, U. D. Schwarz, and R. Wiesendanger, Rev. Sci. Instrum. **69**, 221 (1998).

²S. Hembacher, F. J. Giessibl, and J. Mannhart, Appl. Surf. Sci. **445**, 188 (2002).

³T. Vančura, S. Kicin, T. Ihn, M. Bichler, W. Wegscheider, and K. Ensslin, Appl. Phys. Lett. **83**, 2602 (2003).

⁴W. H. J. Rensen, N. F. van Hulst, and S. B. Kämmer, Appl. Phys. Lett. **77**, 1557 (2000).

⁵F. J. Giessibl, H. Bielefeldt, S. Hembacher, and J. Mannhart, Ann. Phys. **10**, 887 (2001).

⁶T. Eguchi and Y. Hasegawa, Phys. Rev. Lett. **89**, 266105 (2002).

⁷F. J. Giessibl, Appl. Phys. Lett. **76**, 1470 (2000).

⁸S. Heike and T. Hashizume, Appl. Phys. Lett. **83**, 3620 (2003).

⁹T. R. Albrecht, P. Grütter, D. Horne, and D. Rugar, J. Appl. Phys. **69**, 668 (1991).

¹⁰K. Akiyama, T. Eguchi, T. An, Y. Fujikawa, Y. Yamada-Takamura, T. Sakurai, and Y. Hasegawa, Rev. Sci. Instrum. **76**, 033705 (2005).

¹¹A. Michels, F. Meinen, T. Murdfield, W. Göhde, U. C. Fischer, E. Beckmann, and H. Fuchs, Thin Solid Films **264**, 172 (1995).

¹²H. Ueyama, Y. Sugawara, and S. Morita, Appl. Phys. A: Mater. Sci. Process. **66**, S295 (1998).

¹³T. Sakurai, T. Hashizume, I. Kamiya, Y. Hasegawa, T. Ide, M. Miyao, I. Sumita, A. Sakai, and S. Hyodo, J. Vac. Sci. Technol. A **7**, 1684 (1989).

¹⁴E. W. Müller and T. T. Tsong, *Field Ion Microscopy: Principles and Applications* (Elsevier, New York, 1969).

¹⁵T. Eguchi, Y. Fujikawa, K. Akiyama, T. An, M. Ono, T. Hashimoto, Y. Morikawa, K. Terakura, T. Sakurai, M. G. Lagally, and Y. Hasegawa, Phys. Rev. Lett. **93**, 266102 (2004).